

## **WIDESPAN MEMBRANE ROOF STRUCTURES: DESIGN ASSISTED BY EXPERIMENTAL ANALYSIS**

**M. Majowiecki**

*IUAV*

*University of Venice, ITALY*

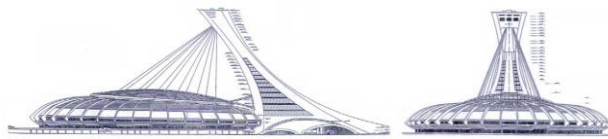
**Key words:** wide span structures , snow and wind loading, experimental analysis, reliability.

**Abstract.** *Wide span structures are today widely applied for sport, social, industrial, ecological and other activities. The experience collected in last decades identified structural typologies as space structures, cable structures, membrane structures and new - under tension - efficient materials which combination deals with lightweight structural systems, as the state of art on long span structural design. In order to increase the reliability assessment of wide span structural systems a knowledge based synthetical conceptual design approach is recommended. Theoretical and experimental in scale analysis, combined with a monitoring control of the subsequent performance of the structural system, can calibrate mathematical modelling and evaluate long term sufficiency of design. Some special remarks concerning the influence on the reliability level of detail design, are given at the end of the paper.*

## 1 INTRODUCTION:

Considering the statistical results of [1], the unusual typologies, materials and the “scale effect” of long span structures several special design aspects arise as:

- the snow distribution and accumulations on large covering areas in function of statistically correlated wind direction and intensity;
  - the wind pressure distribution on large areas considering theoretical and experimental correlated power spectral densities or time histories;
  - rigid and aeroelastic response of large structures under the action of cross-correlated random wind action considering static, quasi-static and resonant contributions;
  - the time dependent effect of coactive indirect actions as pre-stressing, short and long term creeping and temperature effects;
  - the local and global structural instability;
  - the non linear geometric and material behaviour;
  - reliability and safety factors of new hi-tech composite materials;
  - the necessity to avoid and short-circuit progressive collapse of the structural system due to local secondary structural element and detail accidental failure;
  - the compatibility of internal and external restrains and detail design, with the modeling hypothesis and real structural system response;
  - the parametric sensibility of the structural system depending on the type and degree of static indeterminacy and hybrid collaboration between hardening and softening behaviour of substructures.
- In the case of movable structures, the knowledge base concerns mainly the moving cranes and the related conceptual design process have to consider existing observations, tests and specifications regarding the behaviour of similar structural systems. In order to fill the gap, the IASS working group n°16 prepared a state of the art report on retractable roof structures [2] including recommendations for structural design based on observations of malfunction and failures.



---

Figure 1 Montreal Olympic Stadium - A cable stayed roof solution

## 2 SOME WIDE SPAN ENCLOSURES

Due to the lack of space, only some design&analysis illustrations of wide span enclosures, where the author was directly involved, will be included in the present paper with the intention to transmit some experiences that today may be part of the knowledge base.

Long span structures needs special investigations concerning the actual live load distribution and intensity on large covering surfaces. Building codes normally are addressed only to small-medium scale projects. The uncertainties relate to the random distribution of live loads on long span structures imply very careful loading analysis using special experimental analysis.

From the direct author's experience in designing large coverings, the most important experimental investigation regarding live load distribution concerns the snow drift and accumulation factors and the dynamic action of wind loading.

## 2.1 Snow loading experimental analysis on scale models

Olympic Stadium in Montreal. During the design of the new roof for the Montreal Olympic Stadium Figure 1 a special analysis of snow loading was made considering three roof geometries varying the sag of the roof from 10 m, 11.5 m and 13 m., in order to find a minimization of snow accumulation.

The experimental investigation was carried out by RWDI [3] to provide design snow according to FAE (Finite Area Element) method, representing up to day a state of the art on the matter.

The FAE method uses a combination of wind tunnel tests on a scale model and computer simulation to provide the most accurate assessment possible to estimate 30 year snow loads.

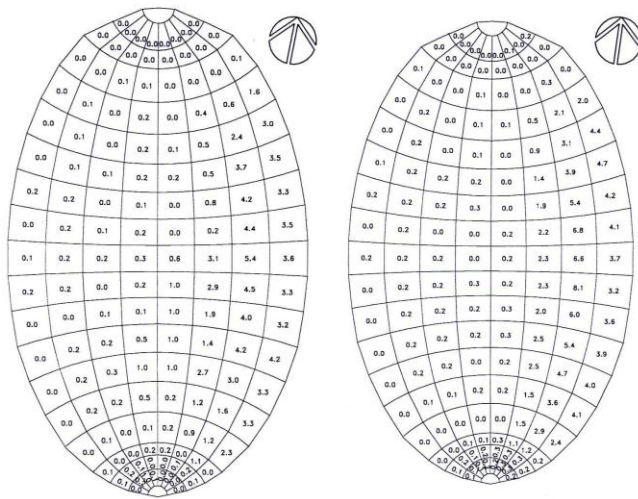


Figure 2 Comparative analysis of snow loading distribution in function of roof shape (10-13m)

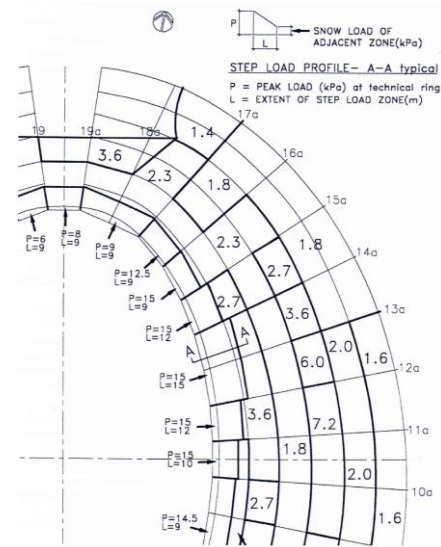


Figure 3 - Sliding and wind snow accumulations step loads

Snow loads depend on many cumulative factors such as, snowfall intensity, redistribution of snow by the wind (speed and direction), geometry of the building and all surroundings affecting wind flow patterns, absorption of rain in the snowpack, and depletion of snow due to melting and subsequent runoff. The current NBCC (National Building Code of Canada) provides minimum design loads for roofs which are based primarily on field observations made on a variety of roofs and on a statistical analysis of ground snow load data. There are, however, numerous situations where the geometry of the roof being studied and the particulars of the site are not well covered by the general provisions of the code. In these situations, a special study, using analytical, computational and model test methods, can be very beneficial since it allows the specific building geometry, site particulars and local climatic factors to all be taken into account. The National Building Code allows these types of studies through its "equivalency" clause and various references to special studies in its commentary.

The model of the three new roof shapes were each constructed at 1:400 scale for the wind tunnel tests. The three model roof designs were each instrumented with 90° directional surface wind velocity vector sensors covering the surface. On the console roof, an additional 90 sensors were installed.

Measurements of the local wind speed and direction, at an equivalent full-scale height of 1 m above the roof surface, were taken for 16 wind directions. The wind speed measurements were then converted to ratios of wind speed at the roof surface to the reference wind speed measured at a height equivalent at full scale to 600 m.

The 30 year ground snow prediction is obtained by interpolation of the data using the Fisher-Typpett type I extreme value distribution method, including both snow and rain ( $S_s + S_r$ ), to be 2.8 kPa, which is in agreement with the code value.

Results of structural load cases and local peak loading, not to be considered as acting over the roof simultaneously are shown in Fig. 2-3. The shape of the roof with a sag of more than 12m. gives separation of the air flow and turbulence in the wake increasing considerably the possibility of snow accumulations. The order of magnitude of the leopardized accumulations in the roof are of 4-15 kN!; local overdimensioning was necessary in order to avoid progressive collapse of the structural system.

## 2.2 Wind loading-experimental analysis on scale models: rigid structures-quasi static behaviour.

The integration of the wind tunnel data into the design process presents significant problems for wide span sub-horizontal enclosures; in contrast to buildings (high rise buildings) where knowledge of the base moment provides a sound basis for preliminary design, there is not single simple measure for the roof. The study of the Stadium of the Alpes and the Rome stadiums [4-5-6] drew attention to the inability of the measuring system employed to provide data in a form that could readily be based as input to the sophisticated dynamic numerical model developed by the designer and lead to discussion between the designer and the wind tunnel researchers to examine alternate techniques that might be used in future projects [7].

The discussions centered on the use of high speed pressure scanning systems capable of producing essentially simultaneous pressure measurements at some 500 points at rates of perhaps 200 Hz per point. With such a system it would be possible to cover in excess of 200 panels and produce a complete description of the load. Such a system would produce roughly 1 to  $2 \times 10^6$  observations for a single wind direction and it is clear that some compression of the data would be required. One possible approach would be to produce a set of load histories,  $Q_j(t)$ , such that:

$$Q_j(t) = \int_A p(x, y, t) \phi_j(x, y) dA \quad (1)$$

where:

$p(x, y, t)$  nett load per unit area at position  $(x, y)$ ;

$\phi_j(x, y)$  weighting function.

For a series of pressure taps of the approximation to  $\phi_j(t)$  would be:

$$Q_j(t) = \sum_{i=1}^N \bar{p}_i(\bar{x}_i, \bar{y}_i, t) A_i \phi_j(\bar{x}_i, \bar{y}_i) \quad (2)$$

$A_i$  area of  $i$ th panel;

$\bar{p}_i$  pneumatic average of pressure at the taps in the  $i^{\text{th}}$  panel;

$\bar{x}_i, \bar{y}_i$  geometric centre of the taps on the  $i^{\text{th}}$  panel;

$N$  number of panels.

The requirements of a system designed to produce the load histories,  $\phi_j(t)$ , is discussed in the following section.

### 2.3 measurement and use of load time histories: *The Thessaloniki Olympic sport complex*

In collaboration with the Boundary layer wind tunnel laboratory of the University of Western Ontario, a new very practical method to obtain the structural response under the random wind action and small displacements (linear response) has been applied under the name of the “orthogonal decomposition method”.

If the weighting functions,  $\phi_j(t)$ , are chosen as mode shapes then  $\phi_j(t)$  is a modal load and its use in conjunction with a dynamic model is clear; either as a set of time histories or a set of modal force spectra and cross-spectra. In the initial stages of a design the roof shape is probably known with reasonable accuracy but mode shapes not so. In such cases it might be appropriate to choose a suitable set of  $\phi_j$  from which modal loads corresponding to shapes  $\psi_i$  can be estimated when the design is more advanced. In such a case we can approximate  $\psi_j$  as:

$$\psi_j \cong \psi_j^i \sum_i^M a_{ij} \phi_j \quad (3)$$

the values of  $a_{ij}$  can be evaluated by minimizing the discrepancy between  $\psi_j$  and  $\psi_j^i$ , ie:

$$\frac{\partial}{\partial a_{ij}} \int \left( \psi_j - \sum_i a_{ij} \phi_i \right)^2 dA = 0 \quad (4)$$

$$i = 1, M$$

If the functions  $\phi_i$  are chosen as a set of orthogonal shapes  $\int \phi_i \phi_j dA = 0; i \neq j$  then the coefficients are given as

$$a_{ij} = \frac{\int \phi_i \phi_j dA}{\int \phi_i^2 dA} \quad (5)$$

For a finite panel sizes the corresponding relationship is:

$$a_{ij} = \frac{\sum_k^N \phi_i(\bar{x}_k, \bar{y}_k) \phi_j(\bar{x}_k, \bar{y}_k) A_k}{\sum_k \phi_i^2(\bar{x}_k, \bar{y}_k) A_k} \quad (6)$$

where:

$$\sum_k^N \phi_i(\bar{x}_k, \bar{y}_k) \phi_j(\bar{x}_k, \bar{y}_k) A_k = 0$$

$$i \neq j$$

The experiment would involve the recording of the local histories  $\psi_j(t)$  from which the model time histories could be constructed and the analysis conducted in either the time or frequency domain (Figures 4-7). For the type of structure under consideration resonant effects are small and the response is largely a quasi-static to a spatially varied load. The deflections induced are closely related to the imposed loads and their distribution differs significantly from the Gaussian form [7]. In such a case the time domain solution, which preserves the extreme value distribution, is to be preferred over a frequency domain approach.

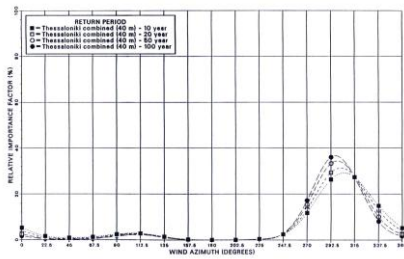


Figure 4 - Relative contribution of Azimuthal Direction to the exceedance probability of various return period wind speeds for Thessaloniki, Thessaloniki, Greece

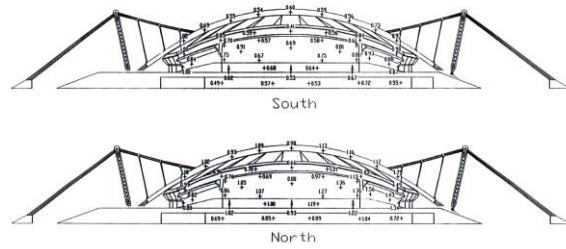


Figure 5 –Taps location

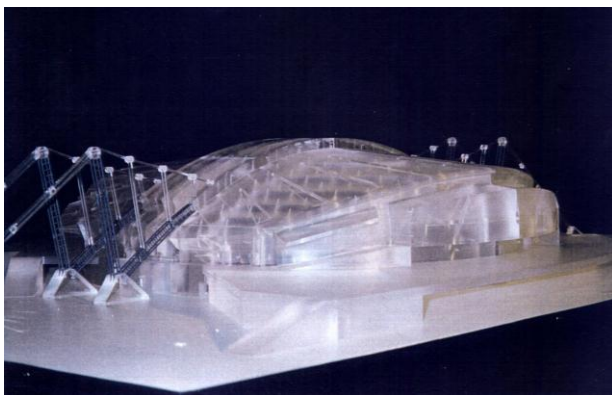


Figure 6 - Views of pressure model

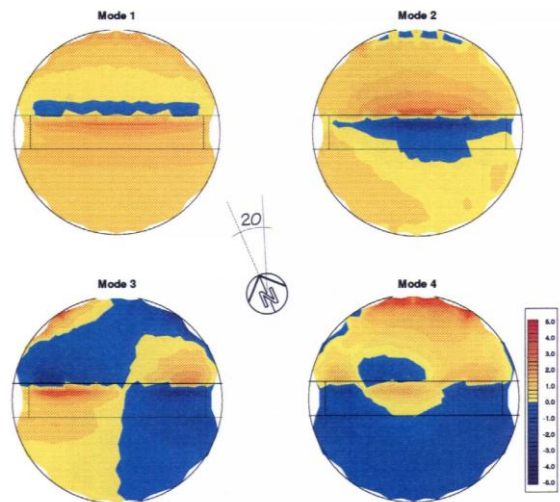


Figure 7 - Orthogonal decomposition: pressure mode shapes

For the seismic analysis a frequency domain approach was adopted. The Kanai-Tajimi PSD was used under the design response spectra prescribed by Eurocode 1; under strong-motion, an acceleration time history was artificially generated according to site and durability characteristics [8].

### 2.3 Wind loading-experimental analysis on scale models : flexible structures-aerodynamic behaviour: *The olympic stadium in Rome*

The wind induced response of the cable supported stadium roof was analysed by a non linear model and a field of multicorrelated artificial generated wind loading time histories [8]. Wind tunnel tests have been carried out at the BLWT Lab. of UWO on a model of 1:200 Fig. 8 scale determining:

- time histories of the local pressures for every 10° of incoming flow direction; the maximum, minimum and average values of the wind pressure have then been evaluated, as well as the root mean square of its fluctuating part;
- pressure coefficients (maxima, minima and average) for every 10° of incoming direction;
- auto and cross-spectra of the fluctuating pressure (averaged on every single panel).



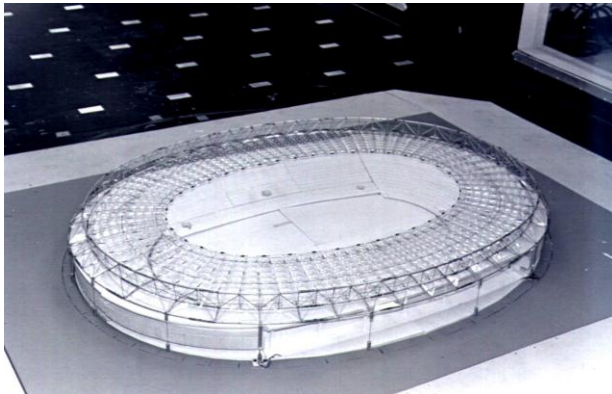


Figure 8 - Aeroelastic model for Rome Olympic Stadium

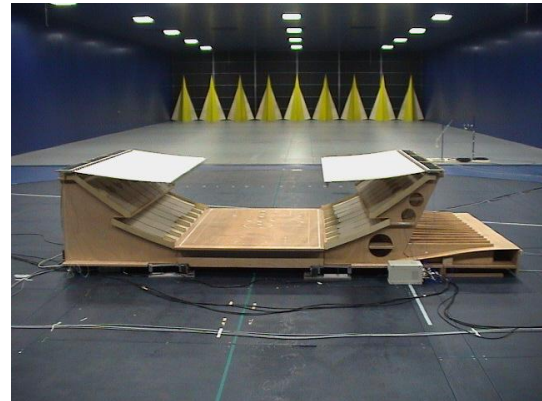


Figure 9 – Aeroelastic model for the Braga Stadium

The aerodynamic behaviour shows a clear shedding phenomenon. The external border of the structure, constituted of the trussed compression ring with triangular section and tubular elements and by the roofing of the upper part of the stands, disturbs the incoming horizontal flow in such a way so that vortex shedding is built up. This causes the roofing structure to be subjected to a set of vortices with a characteristic frequency. This is confirmed by the resulting Power Spectra Density Function of the fluctuating pressures, which shows a peak at about 0.15Hz even if the values rapidly decrease with increasing distance Fig. 10.

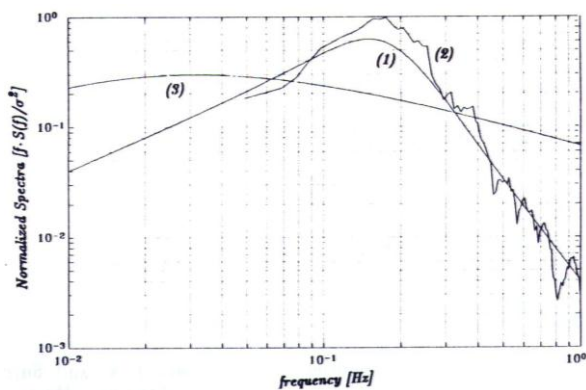


Figure 10 - Target (1), simulated (2) and Kaimal's (3) normalized spectra of wind velocity

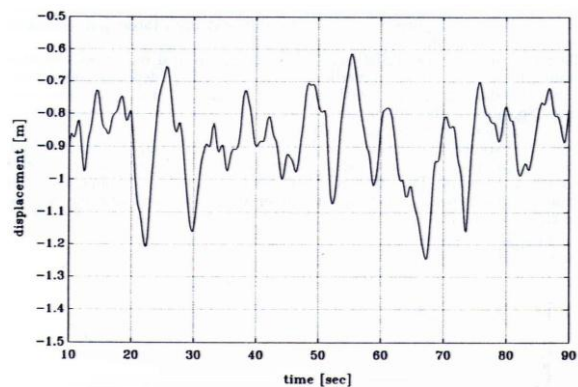


Figure 11 - Time History of the displacement (leeward side at tension ring, run #2)

A fluid-interaction non linear analysis in time domain, made for the checking of La Plata stadium design [9] shows a better agreement between theoretical model and experimental values.

### 3 RELIABILITY ANALYSIS: *the sensibility analysis regarding the new suspended cable roof of Braga (Portugal)*

#### 3.1 Reliability analysis of the roof structural system. Cable strain parametric sensibility.

Considering that in the basic solution the roof will be covered by a long span structural system with

only uplift gravitational stabilization ( Fig.9) it is essential to proceed to the analysis of the response of the structural system to loading patterns and wind induced oscillations.

The analytical process will be organized in order to be controlled by experimental investigations in reduced and full scale.

The reduced scale experimental analysis on rigid and aeroelastic models are concerned with the determination of the dynamic loading on the roof surface and of the stability of the structural system.

The full scale experimental investigations are addressed to check, by a monitoring program, the validity of the global analysis process.

The uncertainties on the elastic modulus of the cable, geometrical and elastic long term creeping, tolerances of fabrication and erection, differences with design prestress, non uniform distribution of temperature, non linear behaviour, created a sensitive response on the suspended roof hanging from a set of suspended cables. The sensibility analysis showed that the response is sensitive to the standard deviation of the cable strain ( $\Delta\varepsilon$ ) variations. The failure probability is given by the probability that an outcome of the random variables ( $\Delta\varepsilon$ ) belongs to the failure domain D. This probability is expressed by the following integral [10]:

$$P_f = \int_{D_f} f_{\Delta\varepsilon}(\Delta\varepsilon) \cdot d\Delta\varepsilon \quad (7)$$

and the most probable failure mechanism will involve primarily the border cables.

The sensibility analysis was, therefore, extremely important to detect the weak points of the structural system and permits proper local dimensioning to prevent chain failure, as illustrated with the failure simulation of same sensitive cable elements.

The roof is composed by a structural concrete plate sustained by  $n$  prestress cables. In the analysis the roof, the bending moments at  $m$  points will be considered. For a particular load combination, the  $n$  cables have computed strains given by the vector  $\varepsilon$ . Considering that these effects are represented by the vector of random variables  $\Delta\varepsilon$  with mean values  $\mu$  and standard variations  $\sigma$ , the problem is to estimate the probability,  $P_f$ , that the generated random bending moments  $M$  will be larger than the plate ultimate resistance moments,  $M_u$ , at any of the  $m$  points of the structural plates system.

### 3.2 Roof structural system data

The following probabilistic description was considered for the random variables  $\Delta\varepsilon$ .

$\mu$  = Vector of mean values of  $\Delta\varepsilon = \mathbf{0}$  (i.e., all possible actions on the cables are considered by the load combination itself).

$\sigma$  = Vector of standard deviations of  $\Delta\varepsilon = \mathbf{0}$ . The  $\sigma$  values were varied from  $0.5 \times 10^{-3}$  to  $0.1 \times 10^{-3}$  so that the sensibility of the system can be studied. These values were selected to cover the range of failure probabilities of practical significance.

$f_{\Delta\varepsilon}(\Delta\varepsilon)$  = Probability density function = Normal distribution with parameters  $\mu$  and  $\sigma$

### 3.3 Failure condition

For load case “i” the bending moments,  $M_x$ ,  $M_y$  y  $M_{xy}$  in the 130 points of the plate can be computed as follow:



$$M_x = M_{Gx_i} + \sum_{j=1}^{34} A_{x_i,j} \cdot \Delta \varepsilon_j \quad M_y = M_{Gy_i} + \sum_{j=1}^{34} A_{y_i,j} \cdot \Delta \varepsilon_j \quad M_{xy} = M_{Gxy_i} + \sum_{j=1}^{34} A_{xy_i,j} \cdot \Delta \varepsilon_j \quad (8)$$

Considering the bending moments in each direction, the failure functions at each point of the plate ( $1 \leq r \leq 130$ ),  $G_r(\Delta \varepsilon)$ , are the following hyperplanes,

$$M_{Upx} - (M_{Gx_i} + \sum_{j=1}^{34} A_{x_i,j} \cdot \Delta \varepsilon_j) < 0 \quad M_{Upy} - (M_{Gy_i} + \sum_{j=1}^{34} A_{y_i,j} \cdot \Delta \varepsilon_j) < 0 \quad (9)$$

$$M_{Unx} - Abs(M_{Gx_i} + \sum_{j=1}^{34} A_{x_i,j} \cdot \Delta \varepsilon_j) < 0 \quad M_{Uny} - Abs(M_{Gy_i} + \sum_{j=1}^{34} A_{y_i,j} \cdot \Delta \varepsilon_j) < 0 \quad (10)$$

$$M_{Uxy} - Abs(M_{Gxy_i} + \sum_{j=1}^{34} A_{xy_i,j} \cdot \Delta \varepsilon_j) < 0 \quad (11)$$

where  $G_r \leq 0$  is failure and  $M_{Uxy}$  is computed from the Johanssen Theory as the smallest of the following expressions

$$M_{Uxy} = (M_{Upx} + M_{Upy}) / 2 \quad M_{Uxy} = (M_{Unx} + M_{Uny}) / 2 \quad (12)$$

In these formulas,  $M_{Upx}$ ,  $M_{Upy}$ ,  $M_{Unx}$ ,  $M_{Uny}$  and  $M_{Uxy}$  are considered always positive.

The failure condition is obtained when failure is reached at any point of the plate, i.e., the structural failure can be defined as

$$(G_1 \leq 0) \cup (G_2 \leq 0) \cup \dots \cup (G_{130} \leq 0) \quad (13)$$

### 3.4 Solution method

Since a closed form solution is not possible for the integral in (7) the failure domain defined by equations above, Montecarlo Simulation must be used. By Montecarlo Simulation, the failure probability is obtained by computing  $G_r(\Delta \varepsilon)$  for several values of  $\Delta \varepsilon$  generated with normal distribution. An approximation to the failure probability is obtained by counting the number of times that  $\Delta \varepsilon$  belong to the  $D_f$  with respect to the total number of simulations. For small failure probabilities, however, direct application of Montecarlo Simulation is not possible because of the large number of needed iterations to get enough accuracy. To avoid this problem, the Orientated Simulation Method was used in this report. A complete description of the method can be found in the paper [10]

### 3.5 Results and conclusions

All the load cases were analysed and the following preliminary conclusions are described as follows.

In order to identify the most dangerous load case the minimum reliability index  $\beta$  for each load cases were calculated for a standard deviation  $\sigma = 0.5 \times 10^{-3}$  for  $\Delta \varepsilon$  of all cables. In Appendix III are shown the distribution of  $M_x$ ,  $M_y$ ,  $M_{xy}$  and  $\beta$  for each load case and for that standard deviation. The following table summarizes the

**Table of**

Load Case	Beta	Phi(-Beta)
1	5.8739	2.14E-09
2	5.7957	3.42E-09
3	5.9555	1.31E-09
4	5.5733	1.26E-08
5	4.1218	1.87E-05
6	4.8436	6.41E-07
7	1.6658	4.79E-02
8	5.7281	5.11E-09
9	5.5396	1.53E-08
10	2.6269	4.31E-03
11	2.3812	8.63E-03
12	4.3046	8.37E-06
13	4.3045	8.37E-06
14	5.8201	2.96E-09
15	5.7479	4.55E-09
16	5.8415	2.61E-09

index  $\beta$  (computed with  $\sigma = 0.5 \times 10^{-3}$ ).

The load cases 7, 9 and 10 have the lowers  $\beta$ , i.e., the higher failure probability, and therefore they are the critical load condition. Particularly critical is the load case 7.

### 3.5 Failure probability and sensibility analysis

The figure 12, shows the failure probability for load combination 7 as a function of the standard deviation,  $\sigma$ , of the cable strain variations,  $\Delta\varepsilon$ .

- The problem is extremely sensitive to the standard deviation,  $\sigma$ , of the cable strain variations,  $\Delta\varepsilon$ . For example for load case 7, if  $\sigma$  is increased from  $2 \times 10^{-4}$  to  $3 \times 10^{-4}$ , Pf is increased from  $2 \times 10^{-5}$  to  $480 \times 10^{-5}$ .
- Cable standard deviation,  $\sigma$ , should be maintained below  $2 \times 10^{-4}$  for the designed ultimate bending moment.
- Larger cable standard deviation,  $\sigma$ , could be allowed increased the slab reinforcement along x-direction in the critical roof zone.

The figure 13, shows the most probable values of  $\Delta\varepsilon$  ( $\times 10^{-3}$ ) in each cable at failure for load combination 7.

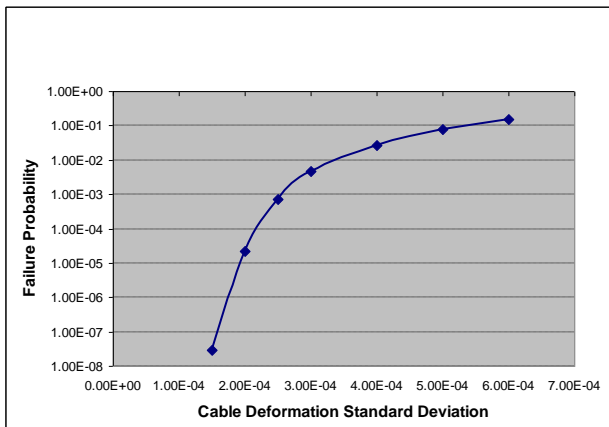


Figure 12 – Failure probability in function of cable deformation standard deviation

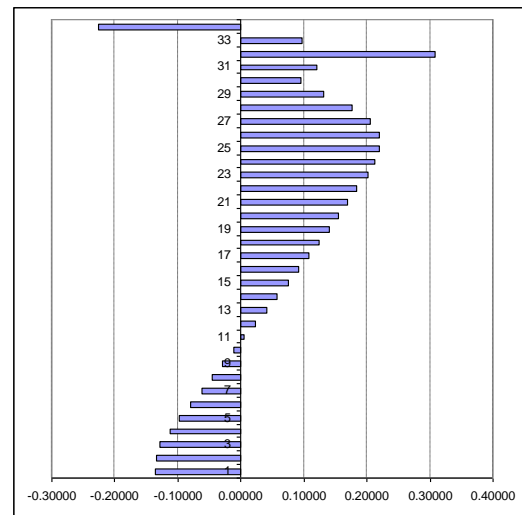


Figure 13 - Predicted 50 year return period peak differential pressures

The following comments can be done.

- The most probable values of  $\Delta\varepsilon$  are practically independent of the standard deviation  $\sigma$ . In other words, the configuration at failure is constant. This configuration is reached with more probability as the standard deviation of  $\Delta\varepsilon$  increases.
- The most probable configuration at failure is mainly due to variations in the strains of cables 32 and 34. Since elongations of cables can be computed as  $\Delta L = L \Delta\varepsilon$ , the elongation at failure of cables 32 and 34 are approximately  $\Delta L_{32} = 210\text{m} \times (-0.2 \times 10^{-3}) = 4.2 \text{ cm}$  and  $\Delta L_{34} = 210\text{m} \times (0.3 \times 10^{-3}) = 6.3 \text{ cm}$ .

## CONCLUSIONS

It has been noted the influence of knowledge base on conceptual design in removing gross human intervention errors from initial design statements.

Design assisted by experimental investigation is a useful integration of the design process of wide span structures.

Sensibility analysis is an extremely powerful tool to determine the influence of parametric design uncertainties for unusual long span structural systems.

## REFERENCES

- [1] R.E. Melchers: Structural reliability, Elley Horwood ltd. 1987.
- [2] Structural Design Of Retractable Roof Structures, IASS working group n°16, WIT Press, 2000
- [3] RWDI: Roof snow loading study-roof re-design Olympic Stadium Montreal, Quebec. Report 93-187F-15, 1993.
- [4] M. Majowiecki: Observations on theoretical and experimental investigations on lightweight wide span coverings, International Association for Wind Engineering, ANIV, 1990.
- [5] B.J. Vickery, M. Majowiecki: Wind induced response of a cable supported stadium roof. Journal of Wind Engineering and Industrial Aerodynamics, 1992, pp. 1447-1458,
- [6] B.J. Vickery: Wind loads on the Olympic Stadium - orthogonal decomposition and dynamic (resonant) effects. BLWT-SS28A, 1993.
- [7] M. Majowiecki: Snow and wind experimental analysis in the design of long span sub-horizontal structures, J. Wind Eng. Ind. Aerodynamics, 1998.
- [8] M. Majowiecki, F. Zoulas, J. Ermopoulos: "The new sport centre in Themi Thessaloniki": conceptual design of the structural steel system, IASS Congress Madrid, september 1999.
- [9] M. Lazzari, M. Majowiecki, A. Saetta, R. Vitaliani : "Analisi dinamica non lineare di sistemi strutturali leggeri sub-orizzontali soggetti all'azione del vento", 5° Convegno Nazionale di Ingegneria del vento, ANIV; Perugia 1998.
- [10] A.G. Puppo, R.D. Bertero, : "Evaluation of Probabilities using Orientated Simulation", Journal of Structural Engineering, ASCE, Vol. 118, No. 6, June 1992.